Journal of
Synchrotron
Radiation

ISSN 0909-0495

Received 6 July 2010
Accepted 28 September 2010

Potassium doping effect on the lattice softening and electronic structure of $Ba_{1-x}K_xFe_2As_2$ probed by X-ray absorption spectroscopy

J. Cheng,[a,b] W. S. Chu,[b]* G. Wu,[c] H. F. Zhao,[b] W. Xu,[b] J. Zhou,[b] L. J. Zhang,[b] X. H. Chen[c] and Z. Y. Wu[a,b]*

[a]National Synchrotron Radiation Laboratory, University of Science and Technology of China, Hefei, Anhui 230029, People's Republic of China, [b]Beijing Synchrotron Radiation Facility, Institute of High Energy Physics, Chinese Academy of Sciences, Beijing 100049, People's Republic of China, and [c]Hefei National Laboratory for Physical Science at Microscale and Department of Physics, University of Science and Technology of China, Hefei 230026, People's Republic of China. E-mail: cws@ihep.ac.cn, wuzy@ustc.edu.cn

$Ba_{1-x}K_xFe_2As_2$ superconducting samples (x = 0, 0.2, 0.4, 0.5) were synthesized by the solid-state reaction method. In this contribution the doping effect of potassium on the lattice dynamics in this newly discovered $Ba_{1-x}K_xFe_2As_2$ superconductor has been investigated by extended X-ray absorption fine-structure spectroscopy. The analysis shows that with potassium doping an increased disorder in the iron layers is mainly related to the softening of the Fe—Fe bond. Information about the electronic structure of these materials has also been obtained by looking at the X-ray absorption near-edge structure spectra that point out the presence of holes in the Fe-3*d*/As-4*p* hybridized orbital of the $BaFe_2As_2$-based system.

Keywords: EXAFS; XANES; $Ba_{1-x}K_xFe_2As_2$.

1. Introduction

The discovery of iron-based superconductors (Chen, Wu *et al.*, 2008; Kamihara *et al.*, 2008; Takahashi *et al.*, 2008) in 2008 represents a real breakthrough, two decades after the copper-based high-T_c superconductors (HTSC) (Bednorz & Müller, 1986), and suggests new research opportunities in this field (Chen, Tesanovic *et al.*, 2008; Chiao, 2008; Grant, 2008). At present we cannot foresee whether the superconducting temperature T_c in these iron-based systems will continue to grow as fast as for the cuprates; however, this unexpected discovery would certainly be useful to improve our understanding of high-T_c superconductors, one of the main open problems of modern physics. The first and probably most urgent question to answer regards the superconducting mechanism of iron-based superconductors: is it the same as copper-based materials due to the many similarities? Actually both cuprates and iron-based superconductors are layered systems and the FeAs layer which is separated by the ReO (Re = La, Sm, *etc.*) or R (R = Ba, Sr, *etc.*) charge reservoir layers is considered as the superconductive layer, like the characteristic CuO_2 layer in cuprates. Finally, the phase diagram of both systems (Chen *et al.*, 2009; Kobayashi *et al.*, 2002) exhibits the competition between antiferromagnetism and superconductivity. Owing to the above considerations, almost all studies have been focused on the structural, electronic and magnetic behaviours revealing many important physical properties. Still, a satisfactory understanding of the pairing mechanism is far from being achieved (Ishida *et al.*, 2009; Sadovskii, 2008). At the same time, a recent observation of a large iron isotope effect in iron-based superconductors (Liu *et al.*, 2009) pointed out that superconductivity in these new materials may be much different from that in cuprate superconductors. As a consequence we have to carefully investigate the possible role of the lattice dynamics in the superconducting mechanism of these iron-based systems.

In the present paper we focus on the potassium doping effects on the lattice dynamics, as well as the partial electronic structure of the $BaFe_2As_2$ system, one of the reference iron-based superconductor materials. We measured both Fe and As K-edge X-ray absorption spectroscopy (XAS), which is an important element-selective tool capable of investigating the local lattice and electronic structure of high-T_c cuprates and other HTSC-related systems (Chu *et al.*, 2009; Wu *et al.*, 1998). Similar to the iron-oxypnictide LaOFeAs, $BaFe_2As_2$ crystallizes in the tetragonal $ThCr_2Si_2$-type structure, composed of alternating $(Fe_2As_2)^{2-}$ and Ba^{2+} layers. The parent compound $BaFe_2As_2$ shows an anomaly in resistivity at about 140 K and exhibits no superconductive property, owing to the structural phase transition from tetragonal to orthorhombic symmetry

(Rotter, Tegel, Johrendt *et al.*, 2008). Potassium doping leads to the suppression of this anomaly in resistivity and induces a superconducting transition at 38 K (Wu *et al.*, 2008). In the $BaFe_2As_2$ parent compound, barium atoms transfer two electrons to the FeAs double layers, maintaining the charge neutrality. Replacement by potassium reduces the number of electrons in the barium layer so that not enough electrons can be transferred to the FeAs double layers and holes appear in the FeAs layers. XANES (X-ray absorption near-edge structure) spectra identify the location of these holes in the Fe-3*d*/As-4*p* hybrid orbital. By analysis of both Fe and As *K*-edge EXAFS (extended X-ray absorption fine structure) spectra it appears that the disorder in the iron layers increases with the amount of potassium. Moreover, temperature-dependent EXAFS spectra confirm a softening of Fe—Fe bonds in the potassium-doped sample.

2. Experiments

Polycrystalline samples $Ba_{1-x}K_xFe_2As_2$ (x = 0, 0.2, 0.4, 0.5) were synthesized by conventional solid-state reaction methods (Wu *et al.*, 2008). We collected both Fe and As *K*-edge XAS spectra of $Ba_{1-x}K_xFe_2As_2$ at room temperature in the transmission mode at the U7C beamline of the National Synchrotron Radiation Laboratory (NSRL), as well as at the BL14W1 beamline of the Shanghai Synchrotron Radiation Facility (SSRF). The electron-beam energy of the NSRL ring is 0.8 GeV with a maximum stored current of about 300 mA, while the electron-beam energy of the SSRF ring is 3.5 GeV with a maximum current of 300 mA. Temperature-dependent Fe and As *K*-edge XAS experiments on $Ba_{1-x}K_xFe_2As_2$ (x = 0 and 0.5) were performed with an accuracy of ±1 K using a Si (111) double-crystal monochromator at the 1W1B beamline of the Beijing Synchrotron Radiation Facility, running at an electron energy of 2.5 GeV with an electron current between 150 and 250 mA. Samples were ground into fine powders then brushed onto tapes that were stacked together to give approximately one X-ray-absorption length (*i.e.* $\mu x \simeq 1$) at their corresponding absorption edges. XAS data were analyzed using *IFEFFIT* (Newville, 2001), and the backscattering amplitudes and phase shifts were calculated using the $BaFe_2As_2$ model cluster (Rotter, Tegel & Johrendt, 2008) of $ThCr_2Si_2$-type using the *FEFF8.2* code (Ankudinov *et al.*, 1998).

3. Discussions and results

3.1. Fe and As *K*-edge EXAFS

Fig. 1 shows Fe and As *K*-edge EXAFS oscillations of the $Ba_{1-x}K_xFe_2As_2$ system extracted from XAS spectra. All EXAFS oscillations have been weighted by k^2 to highlight the region at high k. EXAFS oscillations are identical in shape but exhibit differences in amplitude, especially at the Fe *K*-edge owing to the different potassium doping levels. These differences could be better appreciated by looking at the Fourier transforms (FTs) of the EXAFS shown in Fig. 2, which provide real-space information. We have to underline the fact that the positions of the peaks in the FTs are shifted a few tenths of an angstrom from the actual interatomic distances because of the EXAFS phase shift (Rehr & Albers, 2000). The first peak in the FTs of the As *K*-edge EXAFS spectra corresponds to the contribution from the first shell around the As absorber, *i.e.* the four nearest Fe atoms (labelled As–Fe), while that of the Fe *K*-edge EXAFS spectra includes two subshells around the Fe atom, *i.e.* the four nearest As and Fe atoms (labelled Fe–As and Fe–Fe), because of their comparable distances.

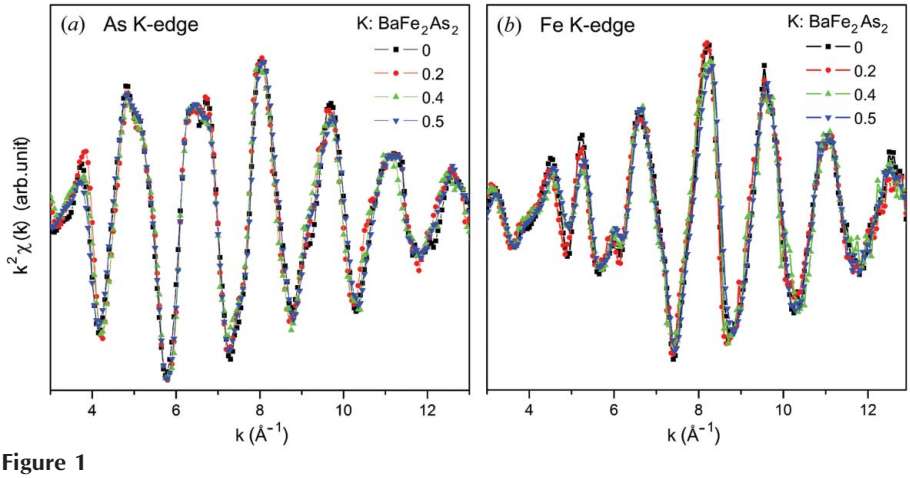

Figure 1
Weighted EXAFS oscillations of the $Ba_{1-x}K_xFe_2As_2$ system at the As *K*-edge (*a*) and Fe *K*-edge (*b*).

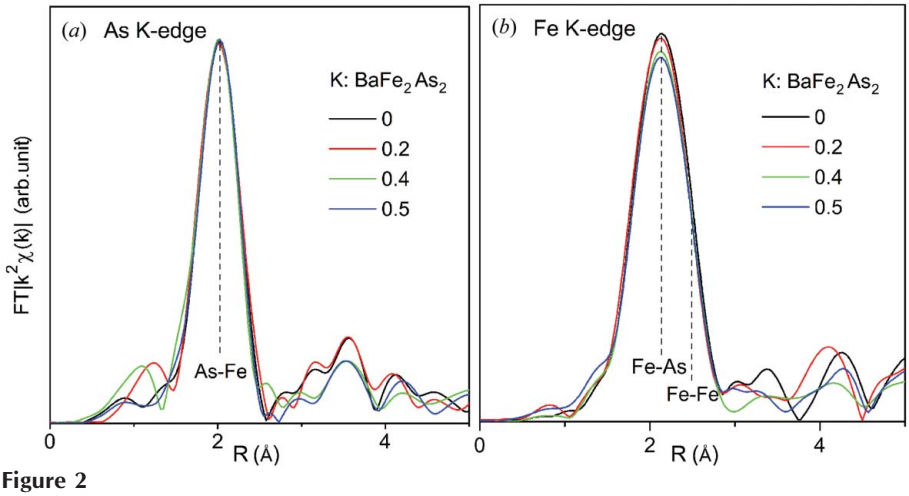

Figure 2
Fourier transforms of the EXAFS spectra of the $Ba_{1-x}K_xFe_2As_2$ systems at the As *K*-edge (*a*) and Fe *K*-edge (*b*).

It can be easily found that both position and intensity of the As–Fe pair in $Ba_{1-x}K_xFe_2As_2$ samples are almost constant. Data point out that this bond is rigid, and both the distance and the mean-square relative displacement of the As–Fe pair are the same. The only change occurs in the intensity of the first peak of the FTs at the Fe *K*-edge EXAFS, *i.e.* the decreasing intensity *versus* potassium concentration. Owing to the identical contributions of the As–Fe and Fe–As pairs the difference may be associated with the Fe–Fe pair suggesting an increased disorder in the iron layers with potassium doping.

In order to obtain quantitative results we fitted the EXAFS spectra of the first peak, which were isolated from the FTs with a rectangular window. The range in k space was 3–13 Å^{-1} and that in R space was 1.4–2.6 Å for the As *K*-edge and 1.4–3.0 Å for the Fe *K*-edge. The number of independent parameters which could be determined by EXAFS is limited by the number of independent data points $N_{\rm ind} \simeq (2\Delta k \Delta R)/\pi$, where Δk and ΔR are the ranges of the fit in the k and R space, respectively. Thus $N_{\rm ind} = 8$ ($\Delta k = 10$ Å^{-1}, $\Delta R = 1.2$ Å) for the As–Fe shell at the As edge, and $N_{\rm ind} = 10$ ($\Delta k = 10$ Å^{-1}, $\Delta R = 1.6$ Å) for the Fe–As and the Fe–Fe shells at the Fe edge, sufficient to obtain all parameters. At first we fit the As edge, fixing the As–Fe coordination number and obtaining the As—Fe distance and the Debye–Waller factor (DWF) $\sigma^2_{\rm As-Fe}$. For the Fe edge we applied two-shells fitting. To reduce the fit variables, the coordination numbers of Fe–As and Fe–Fe, the distance Fe—As and the DWF $\sigma^2_{\rm Fe-As}$ (the same as $\sigma^2_{\rm As-Fe}$, obtained from the As-edge fitting) were fixed, and the corrections to the photoelectron energy origin ΔE were the same for both Fe–As and Fe–Fe shells, leaving the other parameters free.

For the sake of simplicity, Fig. 3 shows only the Fourier-filtered EXAFS signals with the fit of As and Fe *K*-edges of $BaFe_2As_2$ and $Ba_{0.5}K_{0.5}Fe_2As_2$. The results of the EXAFS fit are given in Table 1. Data show a good agreement of the fit with experimental curves both in R and in k space. Owing to the mismatch among the constituent

Table 1
Parameters of the EXAFS fit of the As and Fe *K*-edges for the $Ba_{1-x}K_xFe_2As_2$ system.

R is the mean interatomic distance and σ^2 is the mean-squared deviation from R owing to the thermal motion and the static disorder. The ℜ-factor is a standard function defined by the Standards and Criteria Committee of the International XAFS Society, which weights the quality of the fit.

				ℜ-factor (%)	
$Ba_{1-x}K_xFe_2As_2$	Bond type	R (Å)	σ^2 (10^{-3} Å^2)	As edge	Fe edge
$x = 0$	Fe—As	2.38 ± 0.02	4.7 ± 0.3	0.04	0.33
	Fe—Fe	2.76 ± 0.02	8.1 ± 0.5		
$x = 0.2$	Fe—As	2.38 ± 0.02	4.6 ± 0.2	0.03	0.42
	Fe—Fe	2.76 ± 0.02	8.5 ± 0.4		
$x = 0.4$	Fe—As	2.38 ± 0.02	4.8 ± 0.3	0.03	0.38
	Fe—Fe	2.75 ± 0.02	9.8 ± 0.5		
$x = 0.5$	Fe—As	2.38 ± 0.02	4.6 ± 0.3	0.05	0.47
	Fe—Fe	2.75 ± 0.02	10.0 ± 0.7		

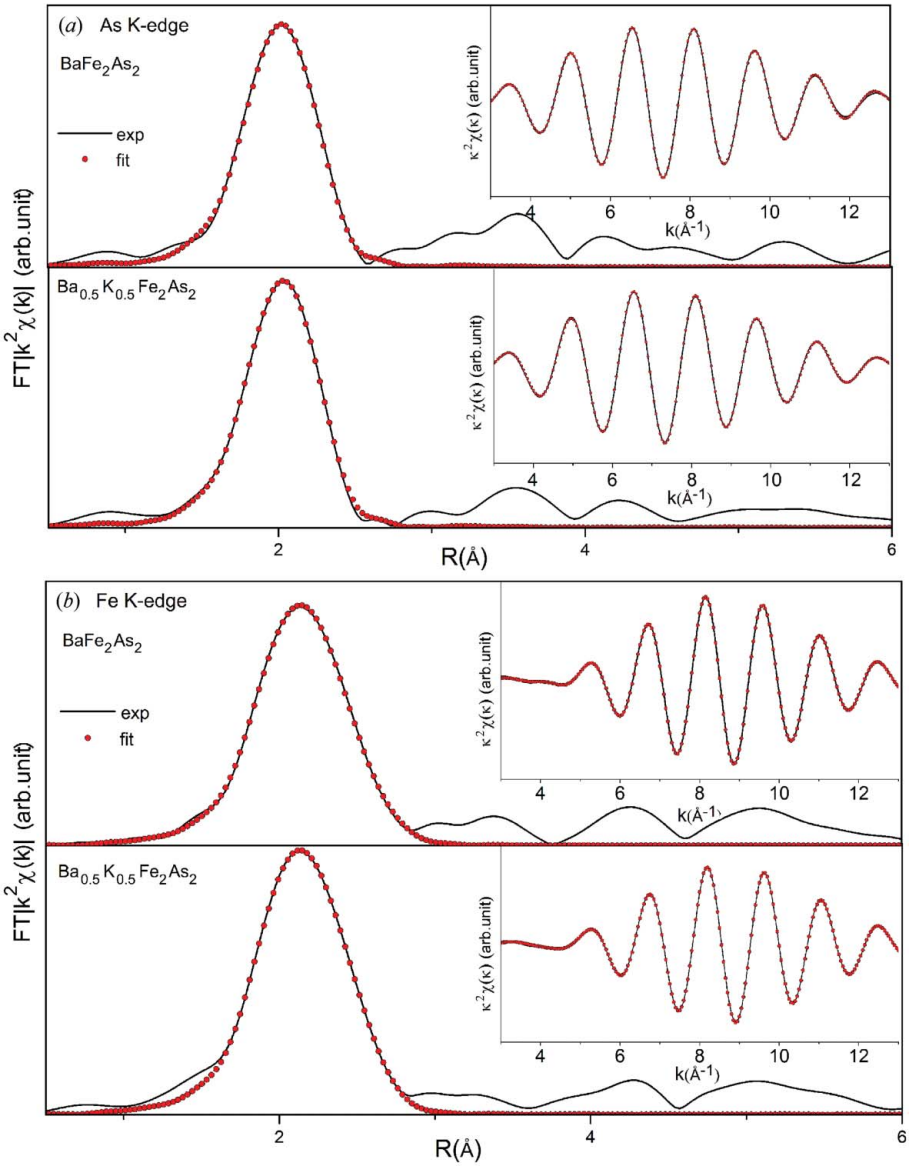

Figure 3
Fourier-filtered EXAFS signal of the first shell at the As *K*-edge (*a*) and Fe *K*-edge (*b*) with the fit in both R and k space (inset) of $BaFe_2As_2$ and $Ba_{0.5}K_{0.5}Fe_2As_2$.

elements and their similar ionic radius [K^+ (1.51 Å) and Ba^{2+} (1.42 Å)], up to 50% potassium doping of both the Fe–As and Fe–Fe pairs exhibit small changes. The small changes in Fe—As and Fe—Fe distances as a function of doping are consistent with the Rietveld refinements of the X-ray powder patterns (Rotter, Pangerl *et al.*, 2008). Potassium doping also affects the behaviour of the DWF σ^2, measuring the mean-square relative displacement of the photon absorber–backscatterer pairs. The value of $\sigma^2_{\mathrm{Fe-As}}$ does not change with increasing doping level x, while $\sigma^2_{\mathrm{Fe-Fe}}$ increases from 8×10^{-3} to 10×10^{-3} Å^2.

The DWF of each atom pair is the sum of two contributions, *i.e.* $\sigma^2 = \sigma_0^2 + \sigma_{\mathrm{vib}}^2$. σ_0^2 is temperature independent and originates from the static disorder. The second contribution is due to thermal vibrations and can be described by the Einstein model (Knap *et al.*, 1985) as $\sigma_{\mathrm{vib}}^2 = [\hbar^2/(2k_B\mu T_E)]\coth[T_E/2T]$. In this equation, $\hbar$ is Planck's constant, k_B is Boltzmann's constant, μ is the reduced mass of the atom pair, T is the temperature and $T_E = (\hbar/k_B)\omega_E$ is the Einstein temperature which can be utilized to estimate and compare the stiffness of different bonds. Indeed, f, the force constant of a bond, is proportional to the square of the Einstein frequency ω_E ($f = \mu\omega_E^2$), *i.e.* proportional to the square of the Einstein temperature T_E.

To recognize whether the increased disorder of iron layers *versus* potassium doping is static or dynamic, temperature-dependent EXAFS of two $Ba_{1-x}K_xFe_2As_2$ samples ($x = 0$ and 0.5) have been measured. Fig. 4 displays the Fe–As DWFs for $x = 0$ and 0.5 as a function of temperature, supporting the DWFs of the Fe–As pair being almost independent of the doping level. Then Fe *K*-edge EXAFS oscillations and the Fourier transforms at several temperatures are depicted in Fig. 5, while Fig. 6 shows the DWFs of the Fe–Fe pair *versus* temperature for the doped and the parent samples. In general, owing to the gradual weakening of thermal vibrations, $\sigma^2_{\mathrm{Fe-Fe}}$ decreases monotonically when the temperature decreases. In order to resolve the doping effect qualitatively we fit the DWF of the Fe–Fe pair for both $x = 0$ and 0.5 samples using the Einstein model with only two independent parameters (σ_0^2 and T_E). Data demonstrate that the static disorder contribution is almost the same for both doped and parent samples. However, with doping a lower Einstein temperature occurs, indicating a softer Fe—Fe bond in a doped sample that enhances vibrations. On the contrary, an enhancement of the Fe—Fe corre-

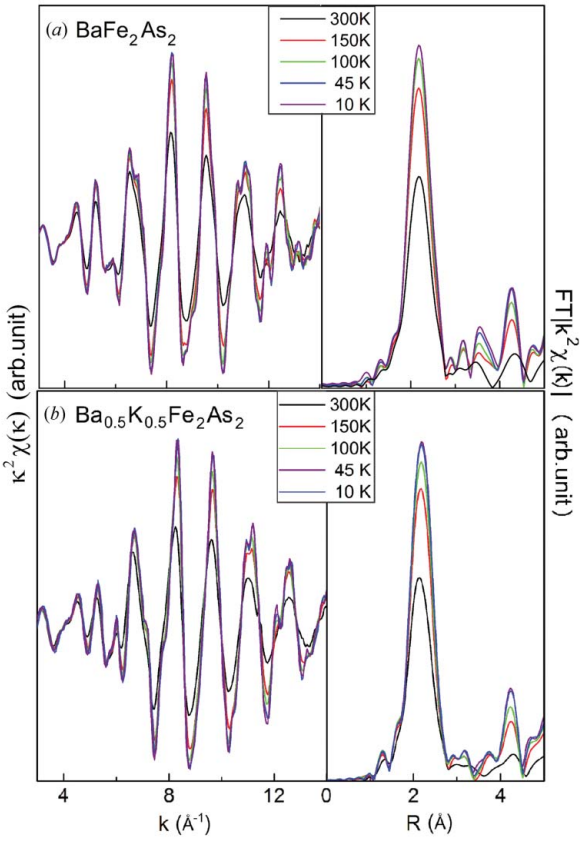

Figure 5
Fe *K*-edge EXAFS oscillations and Fourier transforms at several temperatures for $BaFe_2As_2$ (*a*) and $Ba_{0.5}K_{0.5}Fe_2As_2$ (*b*).

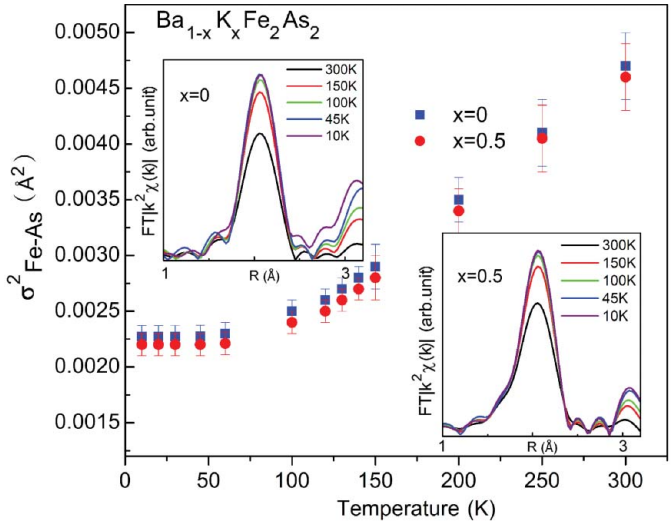

Figure 4
Temperature-dependent DWFs of the Fe–As pair for the $Ba_{1-x}K_xFe_2As_2$ ($x = 0$ and 0.5) samples. The insets show the magnitude of the Fourier transforms at several temperatures.

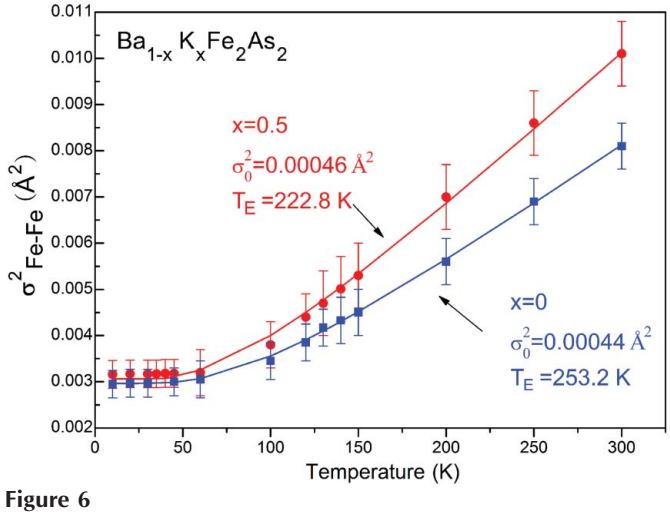

Figure 6
Temperature-dependent DWFs (symbols) of the Fe–Fe pair for the $Ba_{1-x}K_xFe_2As_2$ ($x = 0$ and 0.5) samples and their simulations using the classical Einstein model (solid lines).

lation is displayed in F-doped LaOFeAs (Tyson *et al.*, 2009), so we speculate that the character of the carriers (*i.e.* hole or electron) may play a great role in determining the variation of Fe—Fe correlations.

The correlation between doping and disorder in the iron layers is similar to the structural phase transition observed in the $BaFe_2As_2$ compound when the temperature reaches T_s (the structural transition temperature) at 140 K. $BaFe_2As_2$ undergoes a structural transition and shows a spin-density-wave (SDW) anomaly whose main change is a split of the Fe—Fe bonds (with a separation of about 0.02 Å) (Rotter, Tegel, Johrendt *et al.*, 2008). Our experiment points out that the perturbations (*e.g.* doping or temperature) mainly affect iron layers. In addition, for the $Ba_{1-x}K_xFe_2As_2$ system, structural transition and superconductivity may coexist at a potassium under-doping level. Until $x \simeq 0.4$, structural transition is completely suppressed, and high-T_c superconductivity appears (Chen *et al.*, 2009). This phenomenon may imply a correlation between potassium doping/structural transition and high-T_c superconductivity. Moreover, combining these results, we may try to interpret the potassium doping mechanism. In the parent compound $BaFe_2As_2$, at $T_s \simeq 140$ K, iron layers undergo a relaxation, *i.e.* the four equal Fe—Fe bonds split into two pairs (Rotter, Tegel, Johrendt *et al.*, 2008). With doping, the relaxation should partly or completely transform to the vibration of the Fe–Fe pair in the iron layers. According to the above EXAFS fit, at a potassium under-doping level, the Fe–Fe vibration is too weak and may only partly compensate the relaxation at T_s. Therefore both a structural transition and poor superconductivity may occur decreasing the temperature, but T_s shifts to low temperature (*i.e.* $T_s <$ 140 K). Up to $x \simeq 0.4$, the vibration of the Fe–Fe pair is so strong as to compensate completely the relaxation of $BaFe_2As_2$ at T_s; therefore the structural transition may be completely suppressed and the good superconductivity appears. Thus, within the framework of this structure relaxation, only compounds characterized by an adequate doping concentration could be good superconductors.

Summarizing, EXAFS fit analysis suggests that lattice mechanisms, in particular the softening of the Fe—Fe bond, may play a great role in $BaFe_2As_2$-based superconductors, in agreement with the significant contribution of the Fe in-plane breathing mode to the high-T_c of iron-based superconductors (Eschrig, 2008). On the other hand, the antiferromagnetic SDW induced by the spin ordering of the Fe plane can coexist with the superconductivity (Chen, Li *et al.*, 2008; Chen *et al.*, 2009), so that the behaviour of the Fe–Fe DWFs (*i.e.* the softening of Fe—Fe bonds and thus the weakening of Fe—Fe correlations) may probably relate to the competition between SDW and superconductivity, supporting the possible important role of magnetic fluctuations to superconductivity mechanisms (Christianson *et al.*, 2008; Reznik *et al.*, 2009). However, whether or not the superconductive mechanism in iron-based superconductors is driven by electron–phonon interaction or magnetic fluctuations, or even both, further experimental and theoretical studies are necessary. Our results provide experimental data on the softening of the Fe—Fe pair which are useful to describe the fundamental properties of iron-based superconductors.

3.2. Fe and As *K*-edge XANES

Fig. 7(*a*) shows the normalized Fe *K*-edge XANES spectra of $Ba_{1-x}K_xFe_2As_2$ (x = 0, 0.2, 0.4, 0.5) samples. In comparison with the data of the parent compound $BaFe_2As_2$, Fe *K*-edge XANES of potassium-doped samples show the same energy position and peak shape. The result indicates that potassium doping in the $BaFe_2As_2$ parent compound does not change the structure of the FeAs double layers significantly, in agreement with the EXAFS fit analysis. Moreover, it also demonstrates that the chemical valence of the iron in the $[Fe_2As_2]^{2-}$ layer is unaltered, *i.e.* Fe^{2+} in the doped samples does not change to Fe^{3+} in order to compensate the loss of the charge in the barium layers.

The potassium doping effect on the partial electronic structure of this system is evident at the pre-edge peak of the Fe *K*-edge XANES at 7106.5 eV. This peak increases in intensity and shifts to a high-energy position. Both changes can be correlated to the presence of holes in the FeAs double layers. Owing to the replacement of Ba^{2+} with K^+, the barium layers do not have enough electrons to supply to the FeAs double layers. The *K*-edge XAS corresponds to the excitation of 1*s* core-level electrons to the 4*p* unoccupied orbital of absorbed atoms while in a tetrahedral symmetry the pre-edge peak at the Fe-edge probes the excitation to unoccupied Fe-

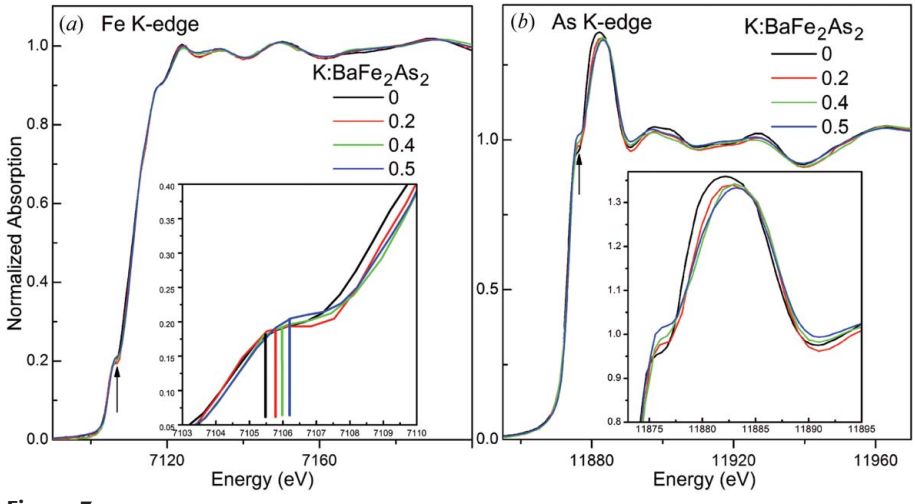

Figure 7
Normalized Fe (*a*) and As (*b*) *K*-edge XANES spectra for the $Ba_{1-x}K_xFe_2As_2$ (x = 0, 0.2, 0.4, 0.5) samples. The arrow in (*a*) shows the excitation of 1*s* core-level electrons to the Fe-3*d*/As-4*p* hybridized orbital in the tetrahedral symmetry (magnified view in the inset); and in (*b*) the arrow shows the increasing intensity (magnified view in the inset) of the shoulder peaks at the As *K*-edge XANES.

3*d*/As-4*p* hybrid bands. Therefore, the increase in the empty density of states and the shift to high energy of the pre-edge peak at the Fe *K*-edge suggest the presence of holes in the Fe-3*d*/As-4*p* hybrid orbital of the $BaFe_2As_2$-based system.

The results are also confirmed by XANES data at the As *K*-edge plotted in Fig. 7(*b*). In these spectra the main peak comes from excitations of 1*s* core-level electrons to a 4*p*-like unoccupied orbital with As-4*d* e_g character (Chang *et al.*, 2009), while the shoulder peak is due to excitations to unoccupied As-4*p*/Fe-3*d* hybrid bands. In the doped samples the shoulder peak at 11875.7 eV of the As edge is higher with respect to that of the parent sample, and the change of the main peak probes the potassium doping effect on the 4*p* orbital of the As atom, in agreement with the hypothesis that holes are shared by iron and arsenic in the $BaFe_2As_2$-based system. The discrepancy in resonance peaks (11900 eV) *versus* doping may be due to different multiple-scattering contributions (Xu *et al.*, 2010) describing the changed medium-range shell around the arsenic atom.

Both Fe and As *K*-edge XANES clearly indicate that hole carriers in $Ba_{1-x}K_xFe_2As_2$ exhibit a Fe-3*d*/As-4*p* character, contrary to the F-doped LaOFeAs system where the charge superconducting carriers have a pure Fe-*d* character (Ignatov *et al.*, 2008). The difference can be correlated to the smaller Fe—As distance and to a corresponding stronger Fe-3*d*/As-4*p* hybridization of the $Ba_{1-x}K_xFe_2As_2$ in comparison with the F-doped LaOFeAs system (Sadovskii, 2008).

4. Conclusion

We applied XAS spectroscopy to investigate potassium doping effects on the lattice dynamics and electronic structure of a new class of superconducting system: $Ba_{1-x}K_xFe_2As_2$. Fe and As *K*-edge EXAFS data indicate that potassium doping may finely tune the local structure. An increasing disorder *versus* potassium concentration appears in iron layers, but the Fe—As bond is rigid. Contrary to the F-doped LaOFeAs system, temperature-dependent EXAFS spectra reveal that with doping the increased disorder is related to the softening of the Fe—Fe bond. What is more, the disorder effect on the T_c of cuprate superconductors has been examined in many studies. All in all, the disorder plays an important role in improving their characteristics and the T_c of these layered superconductors. Furthermore, investigated by XANES, both the pre-edge peak at the Fe *K*-edge and the shoulder peak at the As *K*-edge in potassium-doped compounds exhibit a higher intensity with respect to that of the parent compound. The data point out that the hole carriers in $Ba_{1-x}K_xFe_2As_2$ are shared by both iron and arsenic atoms in the FeAs layers, similar to high-T_c cuprates showing a strong Cu-*d*/O-*p* mixing of superconducting carriers, but different from the F-doped LaOFeAs system where the charge superconducting carriers have a pure Fe-*d* character.

This work was partly supported by the National Outstanding Youth Fund (Project No. 10125523 to ZYW) and by the Knowledge Innovation Program of the Chinese Academy of Sciences (KJCX2-YW-N42). Furthermore, one of the authors, WSC, thanks the National Natural Science Foundation of China (10805055) and the Innovation Fund of the Institute of High Energy Physics (IHEP) for Young Researchers (542009IHEPZZBS50845).

References

Ankudinov, A. L., Ravel, B., Rehr, J. J. & Conradson, S. D. (1998). *Phy. Rev. B*, **58**, 7565–7576.
Bednorz, J. G. & Müller, K. A. (1986). *Z. Phys.* **64**, 189.
Chang, B. C., You, Y. B., Shiu, T. J., Tai, M. F., Ku, H. C., Hsu, Y. Y., Lee, J. F., Wei, Z., Ruan, K. Q. & Li, X. G. (2009). *Phy. Rev. B*, **80**, 165108.
Chen, G. F., Li, Z., Wu, D., Li, G., Hu, W. Z., Dong, J., Zheng, P., Luo, J. L. & Wang, N. L. (2008). *Phys. Rev. Lett.* **100**, 247002.
Chen, H., Ren, Y., Qiu, Y., Bao, W., Liu, R. H., Wu, G., Wu, T., Xie, Y. L., Wang, X. F., Huang, Q. & Chen, X. H. (2009). *Europhys. Lett.* **85**, 17006.
Chen, T. Y., Tesanovic, Z., Liu, R. H., Chen, X. H. & Chien, C. L. (2008). *Nature (London)*, **453**, 1224–1227.
Chen, X. H., Wu, T., Wu, G., Liu, R. H., Chen, H. & Fang, D. F. (2008). *Nature (London)*, **453**, 761–762.
Chiao, M. (2008). *Nat. Phys.* **4**, 446.
Christianson, A. D., Goremychkin, E. A., Osborn, R., Rosenkranz, S., Lumsden, M. D., Malliakas, C. D., Todorov, L. S., Claus, H., Chung, D. Y., Kanatzidis, M. G., Bewley, R. I. & Guidi, T. (2008). *Nature (London)*, **456**, 930.
Chu, W. S., Zhang, S., Yu, M. J., Zheng, L. R., Hu, T. D., Zhao, H. F., Marcelli, A., Bianconi, A., Saini, N. L., Liu, W. H. & Wu, Z. Y. (2009). *J. Synchrotron Rad.* **16**, 30–37.
Eschrig, H. (2008). arXiv:0804.0186 (http://arxiv.org/abs/0804.0186v2).
Grant, P. M. (2008). *Nature (London)*, **453**, 1000–1001.
Ignatov, A., Zhang, C. L., Vannucci, M., Croft, M., Tyson, T. A., Kwok, D., Qin, Z. & Cheong, S. W. (2008). arXiv:0808.2134 (http://arxiv.org/abs/0808.2134v2).
Ishida, K., Nakai, Y. & Hosono, H. (2009). *J. Phys. Soc. Jpn*, **78**, 062001.
Kamihara, Y., Watanabe, T., Hirano, M. & Hosono, H. (2008). *J. Am. Chem. Soc.* **130**, 3296–3297.
Knap, G. S., Pan, H. K. & Tranquada, J. M. (1985). *Phy. Rev. B*, **32**, 2006–2009.
Kobayashi, A., Tsuruta, A., Matsuura, T. & Kuroda, Y. (2002). *J. Phys. Soc. Jpn*, **71**, 1640–1643.
Liu, R. H., Wu, T., Wu, G., Chen, H., Wang, X. F., Xie, Y. L., Yin, J. J., Yan, Y. J., Li, Q. J., Shi, B. C., Chu, W. S., Wu, Z. Y. & Chen, X. H. (2009). *Nature (London)*, **459**, 64–67.
Newville, M. (2001). *J. Synchrotron Rad.* **8**, 322–324.
Rehr, J. J. & Albers, R. C. (2000). *Rev. Mod. Phys.* **72**, 621–654.
Reznik, D., Lokshin, K., Mitchell, D. C., Parshall, D., Dmowski, W., Lamago, D., Heid, R., Bohnen, K.-P., Sefat, A. S., McGuire, M. A., Sales, B. C., Mandrus, D. G., Subedi, A., Singh, D. J., Alatas, A., Upton, M. H., Said, A. H., Cunsolo, A., Shvyd'ko, Yu. & Egami, T. (2009). *Phy. Rev. B*, **80**, 214534.
Rotter, M., Pangerl, M., Tegel, M. & Johrendt, D. (2008). *Angew. Chem. Int. E*, **47**, 7949–7952.
Rotter, M., Tegel, M. & Johrendt, D. (2008). *Phys. Rev. Lett.* **101**, 107006.
Rotter, M., Tegel, M., Johrendt, D., Schellenberg, I., Hermes, W. & Pottgen, R. (2008). *Phy. Rev. B*, **78**, 020503.
Sadovskii, M. V. (2008). *Phys. Uspekhi*, **51**, 1201–1227.
Takahashi, H., Igawa, K., Arii, K., Kamihara, Y., Hirano, M. & Hosono, H. (2008). *Nature (London)*, **453**, 376–378.

Tyson, T. A., Wu, T., Woicik, J., Ravel, B., Ignatov, A., Zhang, C. L., Qin, Z., Zhou, T. & Cheong, S.-W. (2009). arXiv:0903.3992 (http://arxiv.org/abs/0903.3992).
Wu, G., Liu, R. H., Chen, H., Yan, Y. J., Wu, T., Xie, Y. L., Ying, J. J., Wang, X. F., Fang, D. F. & Chen, X. H. (2008). *Europhys. Lett.* **84**, 27010.
Wu, Z., Benfatto, M. & Natoli, C. R. (1998). *Phy. Rev. B*, **57**, 10336–10339.
Xu, W., Joseph, B., Iadecola, A., Marcelli, A., Chu, W. S., Gioacchino, D. Di., Bianconi, A., Wu, Z. Y. & Saini, N. L. (2010). *Europhys. Lett.* **90**, 57001.